

# Andreev Probe of Persistent Current States in Superconducting Quantum Circuits

V. T. Petrushov, K. G. Chua, K. M. Marshall, R. Sh. Shaikhaidarov, and J. T. Nicholls  
*Department of Physics, Royal Holloway, University of London, Egham, Surrey TW20 0EX, UK*

(Dated: November 17, 2018)

Using the extraordinary sensitivity of Andreev interferometers to the superconducting phase difference associated with currents, we measure the persistent current quantum states in superconducting loops interrupted by Josephson junctions. Straightforward electrical resistance measurements of the interferometers give continuous read-out of the states, allowing us to construct the energy spectrum of the quantum circuit. The probe is estimated to be more precise and faster than previous methods, and can measure the local phase difference in a wide range of superconducting circuits.

PACS numbers: 03.67.Lx, 85.25.Cp , 85.25.Dq

Superconducting circuits consisting of loops interrupted by Josephson junctions show persistent current states that are promising for implementation in a quantum computer [1]. Spectroscopy and coherent quantum dynamics of the circuits have been successfully investigated by determining the switching-to-voltage-state probability of an attached superconducting quantum interference device (SQUID) [2]; however, a single switching measurement is low resolution and strongly disturbs both the circuit and the SQUID itself. This revives the fundamental problem of fast high resolution quantum measurements of the persistent current states. The conceptual and technological advance reported here is based on the fact that a persistent current in a quantum circuit is associated with the gradient of the superconducting phase  $\chi$  of the macroscopic wavefunction describing the circuit. The problem of measuring the current reduces to a measurement of the corresponding phase difference  $\theta_q$  across the Josephson junctions.

To measure  $\theta_q$  with a minimum of disruption we use an Andreev interferometer [3, 4]. Our Andreev interferometers, shown in the scanning electron microscope images in Figs. 1a and b, are crossed normal ( $N$ ) silver conductors  $a-b$  and  $c-d$ , with contacts to a pair of superconducting ( $S$ ) aluminium wires at the points  $c$  and  $d$ . The  $N/S$  interfaces play the role of mirrors reflecting electrons via an unusual mechanism first described by Andreev [5]. In Andreev reflection, an electron which is incident on the normal side of the  $N/S$  interface evolves into a hole, which retraces the electron trajectory on the  $N$ -side, and a Cooper pair is created on the  $S$ -side. There is a fundamental relationship between the macroscopic phase of the superconductors and the microscopic phase of the quasiparticles [6]: the hole gains an extra phase equal to the macroscopic phase  $\chi$ , and correspondingly the electron acquires an extra phase  $-\chi$ . This leads to phase-periodic oscillations in the resistance  $R_A$  between the points  $a$  and  $b$  of the interferometer. It should be emphasized that the macroscopic phase is probed by quasiparticles with energies much less than the superconducting gap, so there is no “quasiparticle poisoning” of the superconductor.

We investigate a Josephson quantum circuit with an

attached Andreev interferometer, as shown in Figs. 1a and c. To probe the phase difference within the Josephson circuit, superconducting wires were connected to the points  $e$  and  $f$ , as shown in Fig. 1c. The four-terminal resistance  $R_A$  was measured using the current ( $I_1, I_2$ ) and voltage ( $U_1, U_2$ ) probes shown in Fig. 1b. The oscillating part of the resistance  $\delta R_A$  depends on the superconducting phase difference  $\phi$  between  $c$  and  $d$ , which can be described by [7]

$$\delta R_A = -\gamma \cos \phi, \quad (1)$$

where the amplitude  $\gamma$  is independent of  $\phi$ . The phase difference  $\phi$  can be written [8] as  $\phi = 2\pi \frac{\Phi_A}{\Phi_0} + \theta_q$ , where  $\theta_q$  is the phase difference between the points  $e$  and  $f$  introduced by the lower branch of the Josephson loop. Due to a magnetic field  $B$  applied perpendicular to the plane of the device, the total flux through the interferometer area  $S_A$  (enclosed by  $c-d-e-f$ ) is  $\Phi_A = \Phi_{eA} - L_A I_{SA}$ , where

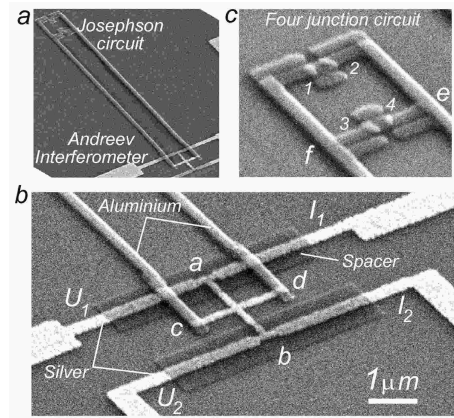


FIG. 1: Layout of Josephson circuit with attached Andreev interferometer. (a) General view. (b) Andreev interferometer consisting of crossed silver wires, connected to the aluminium wires at  $c$  and  $d$ . The resistance  $R_A$  between  $a$  and  $b$  is measured using current ( $I_1, I_2$ ) and voltage probes ( $U_1, U_2$ ). (c) The superconducting quantum loop is interrupted by Josephson junctions at points 1, 2, 3, and 4. There is a superconducting phase difference  $\theta_q$  between  $e$  and  $f$ .

$\Phi_{eA} = S_{AB}$  is the external flux through  $S_A$  which has an inductance  $L_A$ .  $I_{SA}$  is the current circulating in the interferometer loop, and  $\Phi_0$  is the flux quantum  $h/2e$ .

Our Andreev probes were designed according to three criteria:

**I.** To exclude parasitic potential differences between the  $N/S$  interfaces, we fabricate interferometer structures that are symmetric crosses.

**II.** We ensure that the critical current induced in the normal wires (and hence the current  $I_{SA}$  circulating in the interferometer loop) is zero. Thus we exclude both the direct influence of  $I_{SA}$  on the superconducting circuit, as well as the back-action of the measuring current  $I_m$ . According to experimental [9, 10] and theoretical [11, 12, 13] studies the influence of the current through  $a-b$  on the superconductors connected at  $c-d$  vanishes when the critical current is zero.

**III.** To suppress  $I_{SA}$ , but maintain the sensitivity of the conductance to phase, the length  $L_{cd}$  must satisfy the condition  $\xi_N < L_{cd} < L_\phi$ , where  $\xi_N = \sqrt{\hbar D/2\pi k_B T}$  and  $L_\phi = \sqrt{D\tau_\phi}$  are the coherence length and the phase breaking length of the normal metal, respectively;  $D$  is the diffusion coefficient, and  $\tau_\phi$  is the normal metal phase breaking time. The critical current is a thermodynamic property with contributions from quasiparticles within  $k_B T$  of the Fermi energy, and decays within the coherence length. In contrast, the phase coherent conductance is a kinetic property with contributions within the Thouless energy  $E_{Th} = hD/L_{cd}^2$ , and survives up to the order of  $L_\phi$  [7, 14, 15]. In this limit the Josephson circuit phase is given by

$$\theta_q = \phi - 2\pi \frac{\Phi_{eA}}{\Phi_0}, \quad (2)$$

and does not depend on measurement details.

We have tested Andreev probes on three-junction [1] and four-junction Josephson circuits, and have found qualitatively similar behaviour for both circuits. Four-junction circuits allow a symmetric connection to the interferometer, which we believe minimizes the effect of noise currents in the interferometer loop on the quantum states. The devices were fabricated using three-layer electron beam lithography on silicon substrates covered with native oxide. The silver wires of the interferometer are 40 nm thick and 240 nm wide, and the aluminium superconducting wires are 35 nm thick and 360 nm wide. The Josephson circuits are also aluminium, interrupted by  $\text{Al}_2\text{O}_3$  Josephson junctions (Figs. 1 a,c). The spacer was a 30 nm thick  $\text{Al}_2\text{O}_3$  film (Fig. 1b). Resistances were measured using standard low frequency techniques at temperatures between 0.02- 1.2 K.

Figure 2a shows the normalized resistance  $r = \delta R_A/\gamma$  of an interferometer with  $L_{cd} = 2 \mu\text{m}$ , measured as a function of normalized magnetic flux  $\Phi_{eq}/\Phi_0$ , where  $\Phi_{eq} = BS_q$  is the external flux through the Josephson junction loop area  $S_q = 2.45 \times 2.45 \mu\text{m}^2$ . Using a test

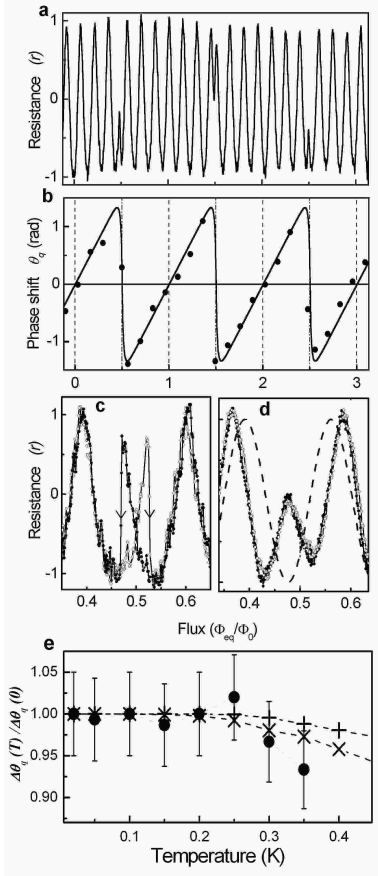


FIG. 2: (a) Normalized oscillating resistance,  $r = \delta R_A/\gamma$ , measured at 20 mK. (b) The phase shift  $\theta_q(\Phi_{eq})$  between  $e$  and  $f$ , as extracted from the oscillations in Fig. 2a; black dots are experimental data and the solid line is calculated using Eqs. 3 and 4. (c) Hysteresis in the resistance at the degeneracy point  $\Phi_{eq} = \Phi_0/2$  in an interferometer attached to a “classical” Josephson circuit, taken with increasing ( $\circ$ ) and decreasing ( $\bullet$ ) magnetic field. (d) Detail of oscillations in Fig. 2a near the degeneracy point  $\Phi_{eq} = \Phi_0/2$ , taken with increasing ( $\circ$ ) and decreasing ( $\bullet$ ) magnetic field. The dashed line corresponds to  $\phi = 2\pi \frac{\Phi_{eA}}{\Phi_0}$ . (e) Experimental temperature dependence of the amplitude of  $\theta_q(\Phi_{eq})$  ( $\bullet$ ), compared to calculations for  $\Delta = 0.035E_J$  ( $+$ ) and  $\Delta = 0.025E_J$  ( $\times$ ).

structure the circulating current  $I_{SA}$  in the interferometer loop was measured to be zero, in agreement with a coherence length in silver of  $\xi_N \leq 1 \mu\text{m}$  (estimated from  $D \approx 100 \text{ cm}^2/\text{s}$ , which was obtained from resistivity measurements). Interference oscillations are measured with a period close to  $\Phi_0$  through the interferometer area  $S_A = 2.45 \times 18.4 \mu\text{m}^2$ . The amplitude  $\gamma$  depends on the resistance  $R_b$  of the  $N/S$  interfaces, reaching values up to  $0.12R_A$  [3]. In this particular device  $R_A = 5 \Omega$  and  $\gamma \approx 0.1 \Omega$ . The measurement current was  $I_m = 1-5 \mu\text{A}$ , and the magnetic flux induced by this current was negligible. Figure 2a shows there are abrupt phase shifts when the flux  $\Phi_{eq}$  corresponds to an odd number of half flux

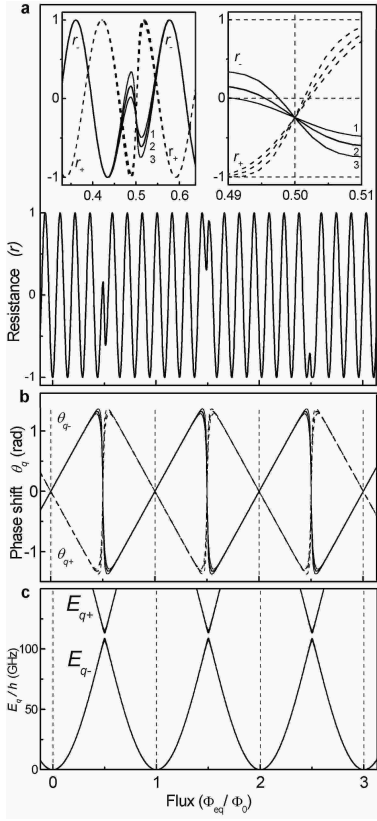


FIG. 3: Calculated fits to the experimental data of Figs. 2a, b and d using Eqs. 3 and 4. (a) Calculated oscillations of the normalized resistance  $r(\Phi_{eq})$  in the ground energy state as a function of the normalized external flux  $\Phi_{eq}/\Phi_0$ . The insets show detail of oscillations in the ground (solid lines) and excited states (dashed lines) for  $\Delta = 0.04E_J$ ,  $\Delta = 0.03E_J$ , and  $\Delta = 0.02E_J$  (curves 1, 2, and 3). (b) Calculated phase shifts  $\theta_-(\Phi_{eq})$  and  $\theta_+(\Phi_{eq})$  in the ground and excited states. (c) The energy spectrum  $E_q$ .

quanta,  $\Phi_{eq}^n = (2n + 1)\Phi_0/2$ , where  $n$  is an integer. The dependence of the phase  $\theta_q$  on magnetic flux is shown in Fig. 2b; the sawtooth structure results from a build-up

of persistent current in the Josephson loop, followed by a transition between states of different circulation.

The shape of the transition at  $\Phi_{eq}^n$  depends on parameters of the Josephson circuit. Figure 2c shows transitions in a circuit with inductance  $L_q \approx 0.5$  nH, and a high critical current,  $I_{cq} \approx 1 \mu\text{A}$ . There is hysteresis associated with the transitions from clockwise to anti-clockwise persistent current states; this is the classical regime where the Josephson energy (and the potential barrier between the persistent current quantum states) is so high that there is no quantum tunnelling at  $\Phi_{eq}^n$ . Figure 2d shows a close-up of the oscillations in Fig. 2a, measured in a Josephson circuit with a lower critical current,  $I_{cq} \approx 0.1 \mu\text{A}$ ; there is a smooth switch from one state to another, with no evidence of hysteresis. Also shown in Fig. 2d is a dashed line that corresponds to  $\phi = 2\pi\frac{\Phi_{eq}}{\Phi_0}$ , which crosses the measured curve  $r(\Phi_{eq})$  at  $\Phi_{eq} = \Phi_0/2$ , the flux at which  $\theta_q = 0$ .

We have measured the influence of the measuring current  $I_m$  on the phase  $\theta_q$ . To within the accuracy of our measurements (less than 5%), the amplitude of  $\theta_q$  is unaffected by currents up to  $I_m = 5 \mu\text{A}$  (corresponding to 25  $\mu\text{V}$  across a-b). High  $I_m$  currents may also induce thermal effects; however, as shown in Fig. 2e the amplitude of  $\theta_q$  is constant over a wide range of temperatures.

Our phase measurements allow us to investigate the energy spectrum of the Josephson circuit. From the equation  $\theta_q = \sin^{-1}\left(\frac{I_{Sq}}{I_{cq}}\right)$ , the phase difference  $\theta_q$  across the Josephson junction is related to the persistent current  $I_{Sq}$  in the Josephson loop;  $I_{Sq}$  is itself related to the energy  $E_q$  of the Josephson loop through the derivative  $I_{Sq} = \frac{\partial E_q}{\partial \Phi_{eq}}$ . Therefore, the equation

$$\theta_q = \sin^{-1}\left(\frac{1}{I_{cq}} \frac{\partial E_q}{\partial \Phi_{eq}}\right) \quad (3)$$

shows that  $\theta_q(\Phi_{eq})$  measurements allow the determination of the energy spectrum  $E_q(\Phi_{eq})$ . To demonstrate the technique, we use a generic form for the spectrum

$$E_q = \frac{\epsilon_q(\Phi_{eq}) + \epsilon_q(\Phi_{eq} - \Phi_0)}{2} \pm \sqrt{\left(\frac{\epsilon_q(\Phi_{eq}) - \epsilon_q(\Phi_{eq} - \Phi_0)}{2}\right)^2 + \Delta^2} \quad (4)$$

where  $2\Delta$  is the energy gap at  $\Phi_{eq} = \Phi_0/2$  between the excited ( $E_{q+}$ ) and ground ( $E_{q-}$ ) states. For energies far away from the degeneracy point  $\Phi_{eq} = \Phi_0/2$ , we take the junction charging energy  $E_c = e^2/2C$  ( $C$  is the junction capacitance) to be much less than the Josephson energy  $E_J$  (test structures show that  $E_J/E_C \approx 10$ , with  $E_J/h \approx 100$  GHz and  $E_C/h = 12$  GHz). Then  $\epsilon_q$  can be modelled

with the two-junction energy  $\epsilon_q = E_J \left[ 1 - \cos \left( \pi \frac{\Phi_{eq}}{\Phi_0} \right) \right]$ , where  $E_J = 2I_{cq}\Phi_0/2\pi$ . To fit our measurements (Fig. 2) of the ground state  $E_{q-}$  there is only one free parameter  $\Delta$ ; we find that  $\Delta = (0.03 \pm 0.005)E_J$  produces the best fit to  $r(\Phi_{eq})$  and  $\theta_q$  over a wide range of flux, as well as generating the energy spectrum  $E_q$  in

Fig. 3c. The model can also describe the temperature dependence of the amplitude of  $\theta_q$  shown in Fig. 2e; the reduction of  $I_{Sq}$  due to thermal fluctuations is given by  $I_{Sq} = I_{Sq}(0) \tanh[(E_{q+} - E_{q-})/2k_B T]$ , and the resulting calculated amplitude of  $\theta_q(T)$  is shown as dashed lines in Fig. 2e for  $\Delta = 0.035E_J$  (+) and  $\Delta = 0.025E_J$  (x).

In anticipation of measurements of the excited states, we use the spectrum  $E_q$  to calculate, see insets of Fig. 3a, the resistance of the ground state  $r_-(\Phi_{eq})$  and excited state  $r_+(\Phi_{eq})$ . When the circuit is irradiated with frequency  $\omega_0 = (E_{q+} - E_{q-})/\hbar$ , the measured voltage is expected to oscillate at the Rabi frequency with an amplitude  $\Delta V_A = I_m(r_+(\Phi_{eq}) - r_-(\Phi_{eq}))$ .

The probe has an operating range from DC to an upper frequency,  $f_0$ , which is limited by the quasiparticle's finite time-of-flight between the N/S interfaces. For our probe  $f_0 \approx D/L_{cd}^2 \approx 10$  GHz. The wide frequency response allows measurements in both the continuous "Rabi spectroscopy" regime [16] and the pulse regime [2, 17]. Note, the Andreev probe measures local phase differences, enabling the direct determination of quantum entanglement between different elements of complicated Josephson circuits, which could be unattainable with previous methods [16, 17]. An increase in the operation speed by orders of magnitude can be achieved using ballistic Andreev interferometers made using a high mobility two-dimensional electron gas (2DEG), which will also allow gate-controlled Andreev probes. Additionally, probes can be fabricated to be impedance matched to standard 50  $\Omega$  or 75  $\Omega$  high frequency setups.

From our measurements we estimate the efficiency of the Andreev probe compared to other methods. The signal-to-noise ratio ( $SNR$ ) for continuous measurements over a frequency range  $\delta f$  is  $SNR = \Delta V_A / \sqrt{S_V \delta f}$ , where  $S_V$  is the spectral density of the voltage noise. With  $R_A = 50 \Omega$ ,  $\Delta R_A = r_+(\Phi_{eq}) - r_-(\Phi_{eq}) = 1 \Omega$ ,  $I_m = 5 \mu\text{A}$ ,  $\delta f \sim 2$  kHz, and with the noise temperature of the cold amplifier  $T_N \approx 1$  K used in [16] we obtain  $SNR = \Delta R_A I_m / \sqrt{4k_B T_N \delta f} \approx 10^3$  for the thermal noise, which is two orders of magnitude larger than previously reported [16].

For the pulse technique an important parameter is the discrimination time  $\tau_m$ , which is the time required to obtain enough information to infer the quantum state. For reflection measurements, the "single shot" measurement time is calculated to be  $\tau_m = S_V / (\Delta V_R)^2$ , where  $\Delta V_R = \frac{\partial V_R}{\partial \Gamma} \frac{\partial \Gamma}{\partial R_A} \frac{\partial R_A}{\partial \theta_q} \Delta \theta_q$  is the reflected signal,  $V_R = \Gamma V_A$ , where  $V_A = I_m R_A$  and  $\Gamma = \frac{R_A - Z_0}{R_A + Z_0}$ . Substituting the cold amplifier noise temperature  $T_N \approx 20$  K used in [17],  $\Delta R_A = \frac{\partial R_A}{\partial \theta_q} (\theta_{q+} - \theta_{q-}) \approx 1 \Omega$ ,  $R_A = Z_0 = 50 \Omega$ ,  $I_m = 5 \mu\text{A}$ , we estimate  $\tau_m \approx 8.8 \times 10^{-7}$  s for the thermal noise - this is more than an order of magnitude shorter than reported in [17].  $\tau_m$  can be further improved using lower noise cryogenic amplifiers. Measurements of the

excited states will reveal the actual decoherence mechanisms. In the mesoscopic interferometer the thermal noise current can be minimized by reducing the number of conducting channels in the length  $L_{cd}$ .

In summary, simple resistance measurements of an Andreev interferometer provide direct read-out of the local superconducting phase difference in quantum circuits; within the accuracy of existing theory there is negligible back-action on the quantum circuit. From the phase  $\theta_q$ , the energy spectrum  $E_q$  can be constructed. The probe is expected to be more precise and faster than previous methods [16, 17], and can measure the local phase difference in a wide range of superconducting circuits. The 2DEG-based Andreev probe can be made gate-controlled. Our probe will allow us to address fundamental aspects of quantum measurements. As the operator of the average phase commutes with the two-state Hamiltonian, measuring the average phase may enable realization of "quantum non-demolition" (QND) measurements [18], possessing important features such as an accuracy that exceeds quantum limits [19].

We thank Yu. V. Nazarov, D. V. Averin, P. Delsing, M. Lea, A. F. Volkov, D. Esteve, D. Vion, H. Pothier, A. Zagoskin, and A. M. van den Brink for valuable discussions. This work was supported by the Engineering and Physical Sciences Research Council (UK).

---

- [1] J. E. Mooij *et al.*, *Science* **285**, 1036 (1999).
- [2] I. Chiorescu *et al.*, *Science* **299**, 1869 (2003).
- [3] V. T. Petrashov, V. N. Antonov, P. Delsing, and T. Claeson, *Pis'ma Zh. Eksp. Teor. Fiz.* **60**, 589 (1994), [*JETP Lett.* **60**, 606 (1994)]; *Phys. Rev. Lett.* **74**, 5268 (1995).
- [4] Y. V. Nazarov and T. H. Stoof, *Phys. Rev. Lett.* **76**, 823 (1996).
- [5] A. F. Andreev, *Zh. Eksp. Teor. Fiz.* **46**, 1823 (1964), [*Sov. Phys. JETP* **19**, 1228 (1964)].
- [6] B. Z. Spivak and D. E. Khmel'nitskii, *Pis'ma Zh. Eksp. Teor. Fiz.* **35**, 334 (1982), [*JETP Lett.* **35**, 412 (1982)].
- [7] V. T. Petrashov *et al.*, *Phys. Rev. B* **58**, 15088 (1998).
- [8] K. K. Likharev, *Dynamics of Josephson Junctions and Circuits* (Gordon & Breach, New York, 1986).
- [9] J. J. A. Baselmans *et al.*, *Nature* **397**, 43 (1999).
- [10] R. Shaikhaidarov *et al.*, *Phys. Rev. B* **62**, 14649 (2000).
- [11] A. F. Volkov, *Phys. Rev. Lett.* **74**, 4730 (1995).
- [12] F. K. Wilhelm *et al.*, *Phys. Rev. Lett.* **81**, 1682 (1998).
- [13] S. K. Yip, *Phys. Rev. B* **58**, 5803 (1998).
- [14] A. F. Volkov and H. Takayanagi, *Phys. Rev. Lett.* **76**, 4026 (1996).
- [15] A. A. Golubov *et al.*, *Phys. Rev. B* **55**, 1123 (1997).
- [16] E. Il'ichev *et al.*, *Phys. Rev. Lett.* **91**, 097906 (2003).
- [17] A. Lupaşcu *et al.*, *Phys. Rev. Lett.* **93**, 177006 (2004).
- [18] V. B. Braginsky and F. Y. Khalili, *Rev. Mod. Phys.* **68**, 1 (1996).
- [19] D. V. Averin, *Phys. Rev. Lett.* **88**, 207901 (2002).